



Electrochemical properties of a new V_2O_5 xerogel

S. MÈGE¹, Y. LEVIEUX¹, F. ANSART¹, J.M. SAVARIAULT² and A. ROUSSET¹

¹LCMIE, Université Paul Sabatier, Bât IIR1, 118 route de Narbonne, 31062 Toulouse Cedex 4, France

²CEMES, rue Jeanne Marvig, 31000 Toulouse, France

Received 10 October 1999; accepted in revised form 1 February 2000

Key words: electrochemical properties, lithium batteries, sol–gel process, surfactant, xerogel

Abstract

Synthesis of $V_2O_5 \cdot 0.2 H_2O$ xerogels by hydrolysis of alkoxide with addition of a surfactant molecule leads to a novel xerogel, which is more amorphous and has a slightly different structure from xerogels prepared by the same method without surfactant. This confers changed lithium insertion properties on the new material. Lithium ions are accommodated at sites different from the sites occupied in xerogels prepared without surfactant. Those new xerogels are able to receive up to almost 2.7 Li/ V_2O_5 ; this represents one more lithium per V_2O_5 than other xerogels. On the other hand, they lose a large proportion of this capacity after the first discharge. The behaviour of the kinetic parameters as a function of lithium content also differs in the two xerogels. This shows that insertion of the first lithium ions in ‘classical’ xerogels is difficult but induces a structural change which makes insertion of further lithium easier. This phenomenon was not observed in the xerogels prepared with surfactant. Furthermore, these present better interfacial properties.

1. Introduction

Electrochemical insertion properties of vanadium pentoxide were studied by Murphy et al. [1]. This compound has attracted attention because its e.m.f. is relatively high (about 4 V vs Li/Li⁺) and it has a layer framework able to accommodate a fairly large amount of lithium. A theoretical intercalation of 4 lithium ions per V_2O_5 is possible, leading to the total reduction of V^{5+} to V^{3+} . This corresponds to a capacity of about 560 mA h g⁻¹ of active cathode material. The corresponding gels have been especially studied during the last two decades with the advent of the sol–gel process [2]. V_2O_5 xerogels based cathodes are attractive materials for use in lithium batteries because they are easier to process for large-scale films and present good electrochemical performances depending on the method used for the preparation. Hibino et al. showed that V_2O_5 can insert reversibly 2.1 lithium per V_2O_5 . More recently, Park et al. [3] showed that it is possible to insert more than 3.3 lithium per V_2O_5 . This corresponds to a surprising capacity of 1150 Wh kg⁻¹. V_2O_5 aerogels were found to have better capacity. Those materials have a great specific surface area around 350 m² g⁻¹ [4]. Le et al. showed that this type of material is able to insert about 4 lithium per V_2O_5 [5]. Their advantage in comparison with crystalline oxide is that during lithium intercalation, their potential remains quite stable because they do not undergo significant phase transition. Furthermore, the sol–gel

route offers the possibility of tailoring the vanadium oxide xerogel properties [6].

V_2O_5 gels are easily made by one of three general routes [7]: (i) pouring molten V_2O_5 into water [8]; (ii) acidification of vanadate salts [9]; (iii) reaction of vanadium alkoxides with water [10]. The present investigation concerns the latter process. The hydrolysis of alkoxide is a very fast reaction due to the electrophilic power of vanadium in these species and to the electronegativity of alkoxo groups [11]. To slow this reaction, we added a surface-active agent during gel synthesis [12]. This also gives better adhesion of the gel to a substrate and, after the elimination of surfactant molecules by a heat treatment, the xerogels have a greater specific surface area. The materials obtained have a structure which is slightly different from the xerogels prepared by the same method but without surfactant which could confer new properties. The structural characterization will be presented later.

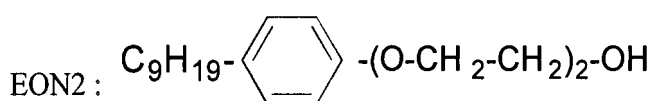
Thus, the fundamental intercalation properties of lithium in V_2O_5 thin films prepared by the sol–gel method both without (XRG: classical xerogel) and with addition of surfactant (XRGs) were compared. In this paper we report the performance of the two materials.

2. Experimental procedure

V_2O_5 gels were prepared by hydrolysis of the vanadium alkoxide $VO(OAm^I)_3$. This alkoxide was synthesized by

reaction of tertioamyl alcohol with commercial V_2O_5 powder (Aldrich). The mixture was heated to $90\text{ }^\circ\text{C}$ under reflux for seven days [13]. The products were purified by distillation under argon at a reduced pressure of 4 mm Hg.

Alkoxide was hydrolyzed by addition of excess demineralized water (pH 5.7) in the molar ratio of 1 vanadium to 80 H_2O . The surfactant was added quickly to the mixture before hydrolysis occurred. The molecule used was a non-ionic surfactant belonging to the nonylphenol family: EON2 (GAF). The quantities of EON2 used to prepared the gel are expressed in molar percent versus $VO(OAm)^3$. The studies were generally done with quantities of EON2 between 10 and 20% EON2.



The mixture was stirred vigorously.

The gel was deposited as thin layers ($1\text{ }\mu\text{m}$ determined by ellipsometry) on gold sheets by dip-coating. The films were then heat treated at $260\text{ }^\circ\text{C}$ for 1 h to remove the surfactant and the other organic molecules. The xerogels obtained whether prepared with or without surfactant were characterized to the stoichiometry $V_2O_5 \cdot 0.2 H_2O$ by thermal gravimetric analysis experiments. Specific surface measurements of thin films were made by mercury porosimetry with an Autopore II 9220 apparatus. The quantities of V^{4+} were evaluated by magnetic measurement of the samples with a Faraday balance made in our laboratory.

The electrochemical tests were done using a conventional three-electrode electrochemical cell in a solution of 1 M $LiClO_4$ in propylene carbonate (Aldrich).

$Li/LiClO_4$ in PC/ V_2O_5 xerogel thin layer

The V_2O_5 xerogels studied here were used as the working electrodes. Lithium metal served as both the reference and the auxiliary electrode. The cells were assembled and tested in an Ar-filled glove box. $LiClO_4$ was vacuum dried at $130\text{ }^\circ\text{C}$ overnight. Measurements of potential versus lithium content were done in near-equilibrium conditions: discharge at a rate of $C/25$ for 1 h and relaxation of the material until $\Delta E < 1\text{ mV}$ for 5 min. The C rate corresponds to the insertion of one Li^+ per V_2O_5 per hour. Cyclic voltammograms were performed with the sweep rate of 5 mV min^{-1} between 3.75 V and 2 V vs Li/Li^+ . Tests were carried out using a Radiometer PGP201 potentiostat/galvanostat at $18\text{ }^\circ\text{C}$. Impedance measurements were done at frequencies of 52 MHz to $10\text{ }\mu\text{Hz}$, using Solartron 1286 electrochemical interface and a Solartron 1260 frequency response analyser. Initially, various d.c. voltages were applied between the working and counterelectrodes until equilibrium was established, enabling ac impedance measurements for different values of x . The amplitude of the applied ac voltage was equal to 10 mV.

3. Results and discussion

3.1. Morphology and composition

Morphology studies of material prepared with and without EON2 showed that XRGs were the more porous material. XRG had a low porosity and surface area below $5\text{ m}^2\text{ g}^{-1}$. On the other hand, the specific surface area of XRGs was about $30\text{ m}^2\text{ g}^{-1}$ for 10% EON2. This value increased with the surfactant content added to the gels and reached $80\text{ m}^2\text{ g}^{-1}$ for 75% of surfactant (Figure 1). The final composition of the xerogels was determined by chemical titration (to determine the quantity of carbon) and by magnetic measurements (to determine the proportion of V^{4+}). About 5 wt % of residual carbon remained after the thermal treatment in

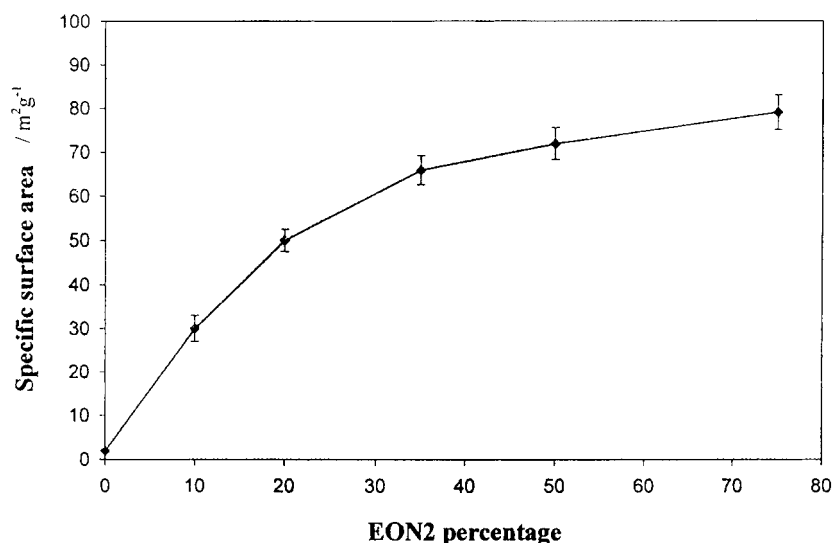


Fig. 1. Specific surface area against percentage of EON2 added during gel synthesis.

XRGS prepared with surfactant. This was independent of the amount of EON2 added but it was smaller in XRG, where the total weight ratio of carbon in the materials was about 1%. The V^{4+} content against EON2 ratio are reported in Table 1. The results show that the nonylphenol surfactant brought about reduction of V^{5+} to V^{4+} . The exact stoichiometry of these xerogels was therefore $V_{2-x}^{5+}V_x^{4+}O_{5-x/2} \cdot 0.2 H_2O$. The two xerogels have a structure close to crystalline V_2O_5 [14]. However, slight differences appear for XRGS. These xerogels have a more dilated structure in the sheets (4% dilatation in y direction and 0.5% in x direction) [15]. Their structural characteristics will be discussed in a latter paper.

3.2. Electrochemical properties

The cyclic voltammograms are shown in Figure 2. They indicate a strong effect of the addition of surfactant on the insertion mechanism. The XRG electrode shows cathodic peaks at 3 V and 2.5 V. Two corresponding anodic current peaks appear at 3.05 V and 2.8 V. In contrast, the XRGS cathodic material shows only one cathodic current peak at 2.5 V with a corresponding anodic peak at 2.7 V. This demonstrates that the intercalation process is not the same in the two materials. The first lithium site at 3.05 V does not exist in XRGS. In the both cases, lithium ions are accommodated at sites different from those in orthorhombic V_2O_5 : the crystalline oxide intercalated with lithium shows peaks at 2.1, 2.3, 3.1 and 3.4 V [16]. The shape of the cyclic voltammogram of the XRGS at low potential indicates a capacitance-like behaviour. Further cyclic voltammograms had the same shape in both cases. This demonstrates that the two xerogel hosts maintained their structure after repeated cycling.

Table 1. Percentage of V^{4+} in xerogels against percentage EON2 used to prepare the gel

Percentage EON2	0%	10%	20%	25%	40%
Percentage V^{4+}	8%	13.5%	18%	21%	31%
(Uncertainty 20%)					

In Figure 3, the near-equilibrium potential E (V vs Li/Li^+) of the two kinds of xerogels are plotted against x , where x is the lithium content in $Li_xV_2O_5 \cdot 0.2 H_2O$. One more lithium ion per V_2O_5 was inserted in XRGS which corresponds to a theoretical specific capacity of 350 Ah kg^{-1} instead of 240 Ah kg^{-1} for XRG electrode material. Furthermore, the two curves do not have the same shape. The $E-x$ diagram of the XRG shows an inflection point at x near 0.75. This indicates that the material is not completely amorphous. In contrast, the discharge curve of the XRGS material is almost linear. The curve obtained for XRG shows a sharp decrease when the potential of the cell reaches about 2.5 V. The lower insertion capacity of these films may be due to the onset of high resistivity in the solid or to the disappearance of intercalation sites at low potential. No such decrease in the $E-x$ curve was observed in the new material obtained with EON2. Thus, their higher insertion capacity results from insertion of lithium below 2.5 V but is not linked to the proportion of EON2 used (in the studied range: 10–20%). As shown in Table 2, the ratio of lithium inserted does not change significantly with the ratio of EON2. This result is surprising because with increasing amounts of EON2, the ratio of V^{4+} vs V^{5+} increases and, thus, the amount of reducible species decreases. Otherwise, structural studies by WAXS show that the structure of the xerogels is not altered by the insertion of Li^+ . In both cases, lithium ions are not totally extracted on subsequent charge cycles. This is illustrated in Figure 4 for

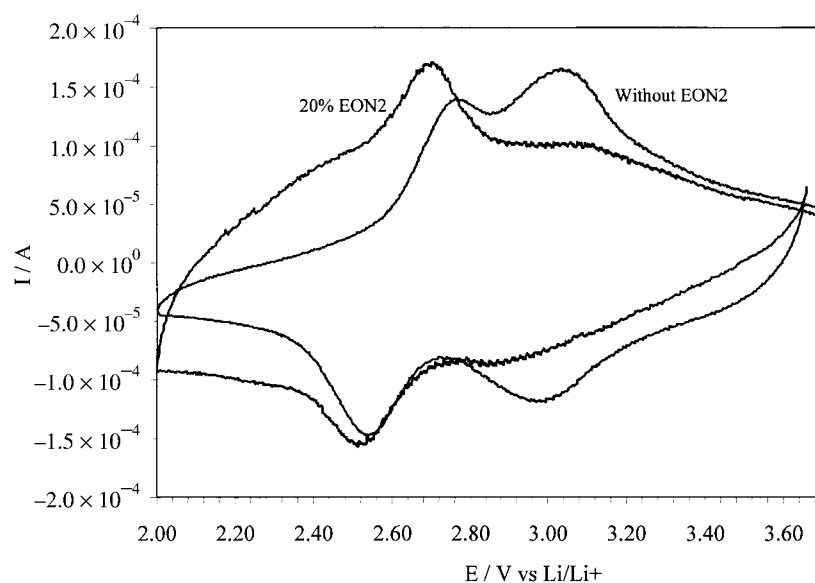


Fig. 2. Cyclic voltammograms of XRG and XRGS. Electrode surface coverage was about 0.2 mg cm^{-2} and thickness $1 \text{ }\mu\text{m}$. Sweep rate 5 mV min^{-1} .

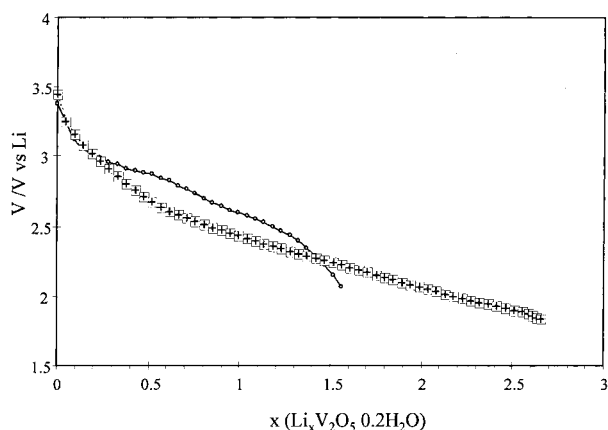


Fig. 3. Potential against lithium composition in XRG and XRGs at 18 °C. Key: (○) 0% EON2 and (■) 20% EON2.

consecutive discharges and charges done at a rate of $C/5$. XRG lost about 30% of their capacity after 20 cycles. This capacity loss was greater in XRGs (about 35%), due to a greater decrease in capacity after the first cycle. Effectively, the decrease in the amount of lithium inserted into the cathode after the first cycle is about 15%. This is possibly due to a passivation phenomenon. After this first cycle, approximately 4% of the capacity is lost per deep discharge cycle for the two xerogels at $C/5$.

The lithium diffusion coefficient and charge transfer resistance were determined as a function of lithium content using complex impedance measurements. Figure 5 shows typical impedance plots as a function of x for XRG and XRGs prepared with 20% EON2. The simulation was done using the spectrum based on a Randles circuit [17]. The time constants of the different processes are well separated. The Nyquist plot of the system reported in the complex plane consists of a semicircle centered on the real axis at high frequencies (corresponding to the interfacial capacity coupled with the charge transfer resistance) and a straight line with an angle of 45 degrees with the real axis (corresponding

Table 2. Percentage of EON2 against lithium insertion rate

EON2/%	x ($\text{Li}_x \text{V}_2 \text{O}_5 \cdot 0.2 \text{H}_2 \text{O}$)
0	1.7
10	2.6
20	2.6
25	2.7

to the semiinfinite diffusion of Li^+ ions according to the Warburg model [18]). From the first part of the plot, both the double-layer capacitance and the charge-transfer resistance can be deduced. The chemical diffusion coefficient D_{Li} may be obtained from the Warburg impedance (Z_w). It is calculated from the equation of the Warburg prefactor $K(Z_w = K\omega^{-1/2})$ which corresponds to the slope of the plots $\text{Re}(Z)$ against $\omega^{-1/2}$.

$$K = \left(\frac{V_m}{(2)^{1/2} Z F D^{1/2} S} \right) \left(\frac{dE}{dx} \right)$$

where V_m is the molar volume ($\text{cm}^3 \text{mol}^{-1}$), dE/dx is the slope of the coulometric titration curve at each x value, S is the electrode area (cm^2).

Numerical values for D , σ (conductivity), R_{ct} (charge transfer resistance) and C_{dl} (double layer capacity) at various compositions x are given in Tables 3 and 4. Figure 6 shows the evolution of D_{Li} for both XRG and XRGs against x . The behaviour of the curves differs depending on the preparation of the xerogel (with or without EON2). For XRG, D_{Li} is first equal to $2.8 \times 10^{-13} \text{cm}^2 \text{s}^{-1}$ for $x = 0$; its value increases for $x = 0.18$ and then decreases with $x > 0.18$. A completely different behaviour is observed concerning the XRGs: for very low values of x , D_{Li} is first relatively high, in the range from 10^{-11} to $10^{-12} \text{cm}^2 \text{s}^{-1}$. But, as x increases, the diffusion coefficient decreases dramatically, reaching $10^{-17} \text{cm}^2 \text{s}^{-1}$. In fact, in XRG, ion diffusion seems to be

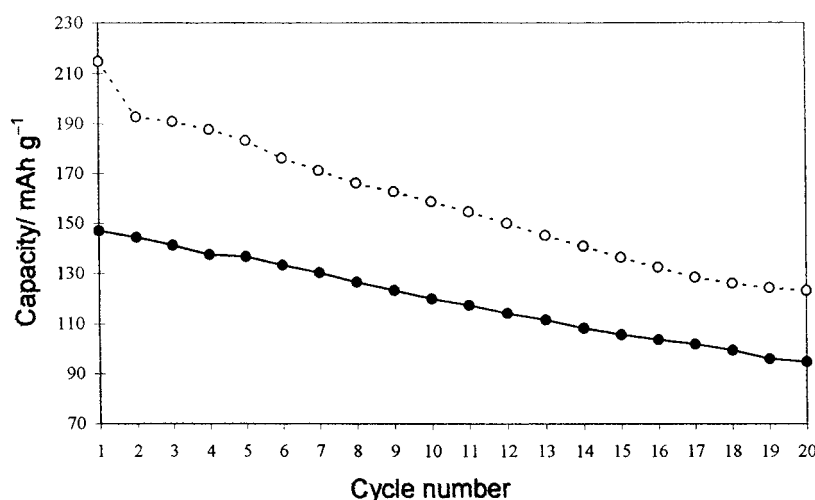


Fig. 4. Charge inserted into XRG and XRGs cathodes as a function of the cycle number for cycling between 4 V and 2 V vs Li/Li^+ at a rate of $C/5$. Key: (●) 0% EON2 and (○) 20% EON2.

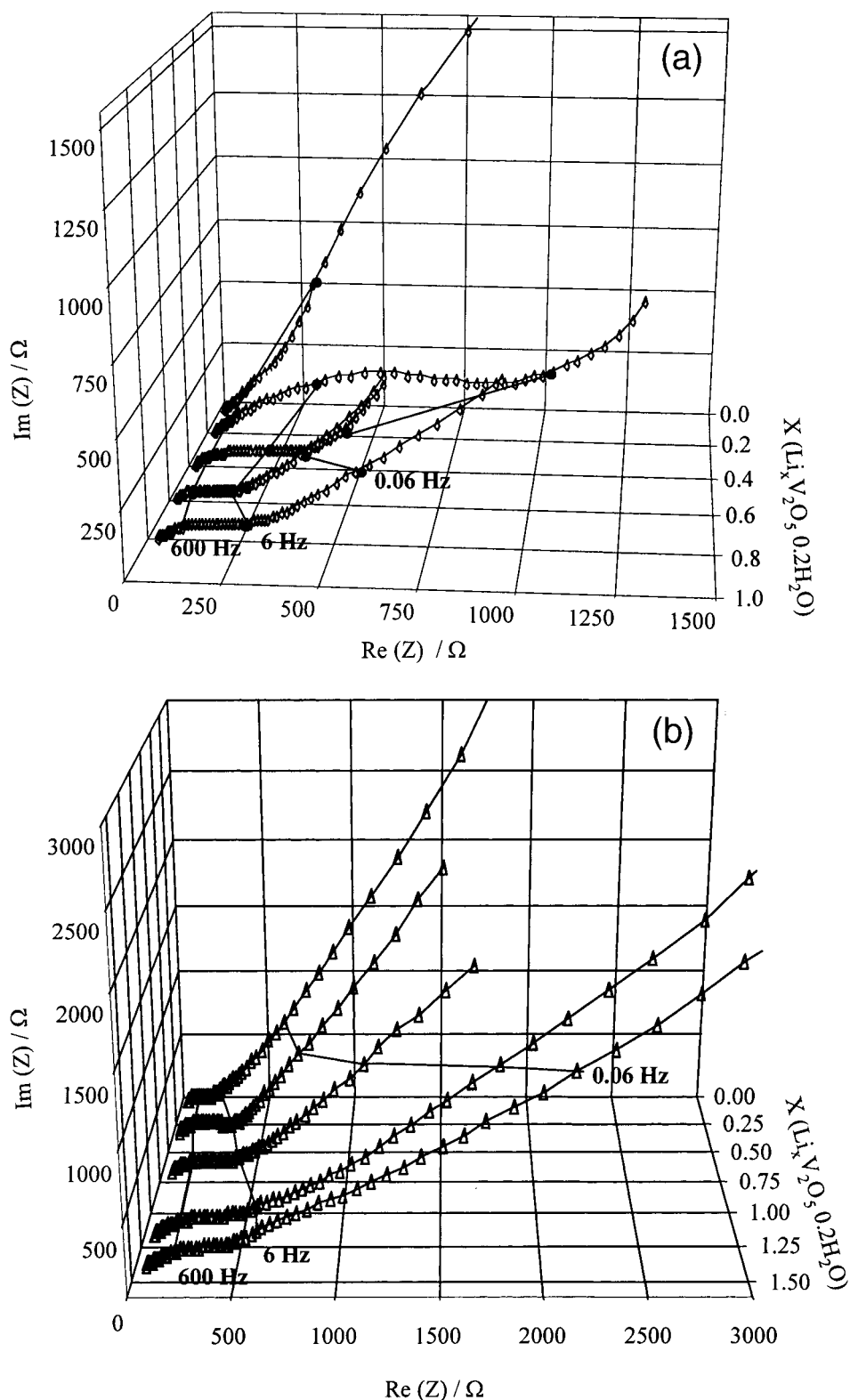


Fig. 5. Complex impedance plots against lithium composition: (a) for XRG and (b) for XRGS.

facilitated by the insertion of a small amount of lithium. This phenomenon is explained by a structural rearrangement (parameter dilatation) provoked by the insertion of the first lithium ions. This behaviour does not exist for XRGS. It can be correlated to a dilated structure previously observed for these xerogels [15]. For $x > 0.4$, diffusion in XRG is faster than in XRGS. This

may be attributed to a higher level of long-range atomic ordering in XRG as evidenced by o.c.v. (open circuit voltage) curves and by structural studies (which will be reported in a later paper). In crystalline V_2O_5 , the values of D_{Li} are higher. They vary between 10^{-7} and $10^{-9} \text{ cm}^2 \text{ s}^{-1}$ [19–21] depending on the lithium ratio in the structure or on the structural phase.

Table 3. Kinetic parameters of XRG for various quantities of lithium inserted
0% EON2

x	E° /V vs Li/Li^+	D_{Li} / $\text{cm}^2 \text{ s}^{-1}$	σ_{Li} / $\Omega^{-1} \text{ cm}^{-1}$	R_{ct} / $\Omega \text{ cm}^2$	$10^6 C_{\text{dl}}$ /F cm^{-2}
0	3.61	2.80×10^{-13}	1.80×10^{-11}	17725	3.10
0.18	3.38	1.57×10^{-12}	3.79×10^{-10}	1884	5.00
0.36	3.13	1.32×10^{-12}	5.11×10^{-10}	728	7.00
0.54	2.79	7.62×10^{-13}	4.32×10^{-10}	110	1.76
0.81	2.67	6.67×10^{-15}	3.13×10^{-11}	132	1.99
1.08	2.6	1.08×10^{-15}	9.43×10^{-12}	149	1.92
1.26	2.57	2.28×10^{-16}	4.72×10^{-12}	155	2.06
1.44	2.56	1.68×10^{-17}	8.20×10^{-13}	187	2.18

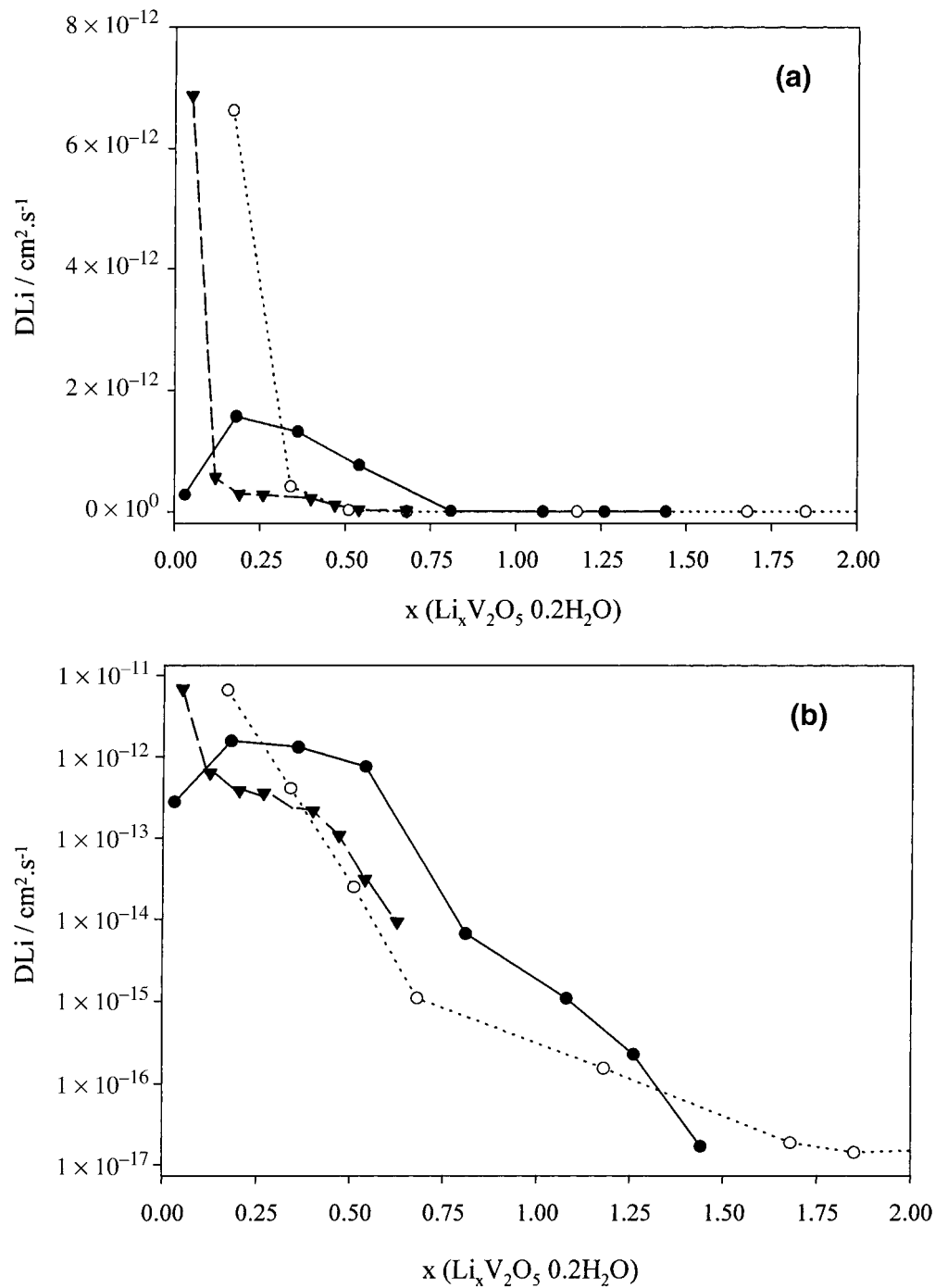


Fig. 6. Values of D_{Li} against lithium composition: (a) linear scale and (b) semilogarithmic scale. Key: (●-●) 0% EON2, (○-○) 20% EON2 and (▼-▼) 10% EON2.

Table 4. Kinetic parameters of XRGs for various quantities of lithium inserted
20% EON2

x	E° /V vs Li/Li ⁺	D_{Li} /cm ² s ⁻¹	σ_{Li} /Ω ⁻¹ cm ⁻¹	R_{ct} /Ω cm ²	$10^6 C_{\text{dl}}$ /F cm ⁻²
0	3.31	2.25×10^{-11}	8.10×10^{-10}	33	1.82
0.17	2.91	6.63×10^{-12}	9.46×10^{-10}	68	2.36
0.34	2.66	4.13×10^{-13}	2.04×10^{-10}	64	2.48
0.51	2.56	2.46×10^{-14}	5.32×10^{-11}	59	2.04
0.68	2.53	1.09×10^{-15}	6.12×10^{-12}	78	1.87
1.18	2.48	1.54×10^{-16}	1.25×10^{-12}	93	2.80
1.68	2.4	1.85×10^{-17}	2.72×10^{-13}	127	2.40
1.85	2.36	1.40×10^{-17}	2.26×10^{-13}	145	2.23
2.02	2.34	4.74×10^{-18}	1.18×10^{-13}	157	2.35
2.19	2.31	8.22×10^{-18}	1.48×10^{-13}	168	3.40

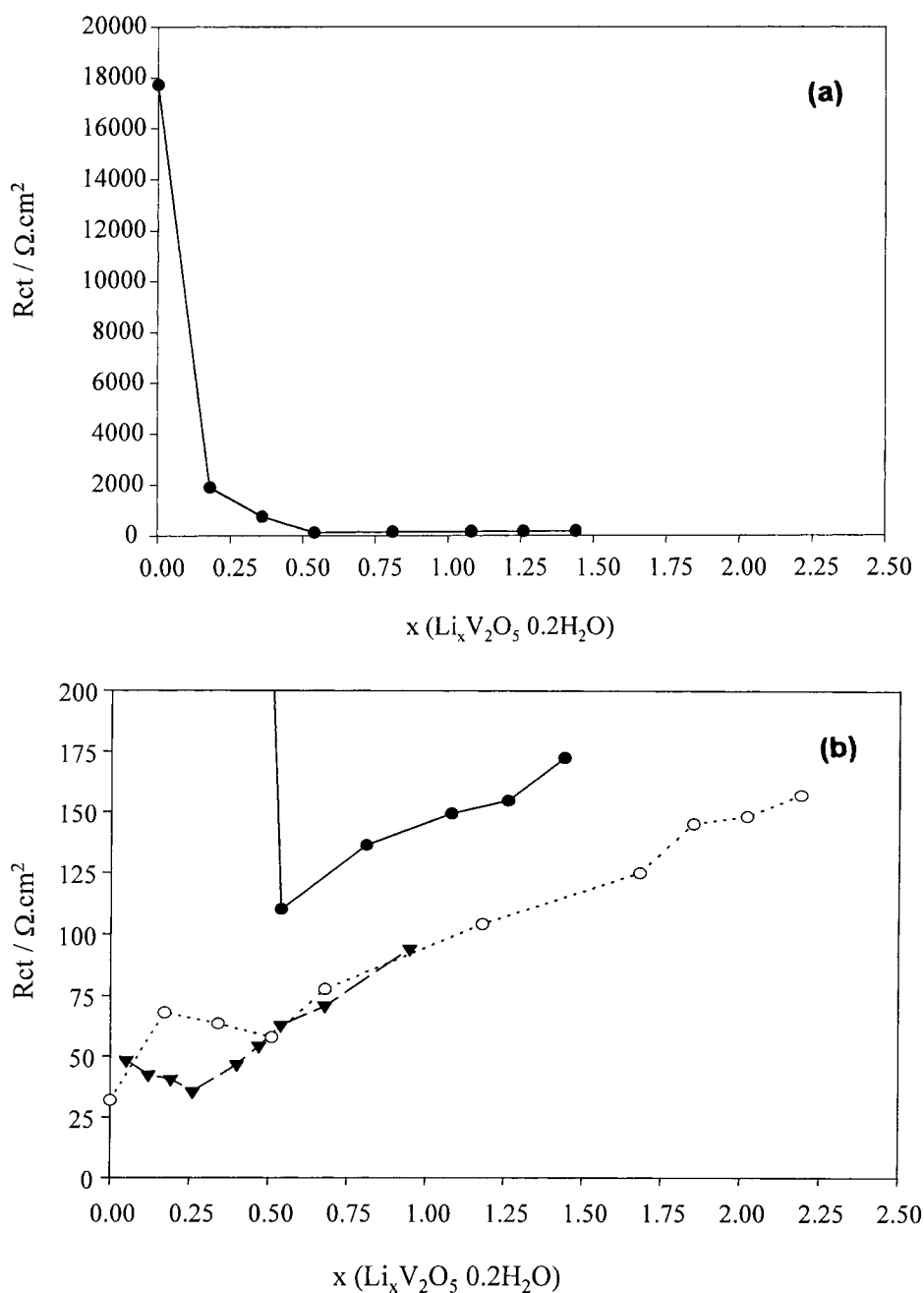


Fig. 7. Values of charge transfer resistance as a function of lithium composition: (a) large scale for XRG and (b) XRG and XRGs. Key: (●—●) 0% EON2 (a and b); (○—○) 20% EON2 and (▼—▼) 10% EON2 (b only).

Interfacial properties are also different, as shown by the change in the charge transfer resistance R_{ct} with x (Figure 7). For XRG, the value of R_{ct} decreases 1000-fold between $x = 0$ and $x = 0.3$. For higher values of x , R_{ct} increases slowly. Additional energy must be supplied to locally distort the network to allow the insertion of the first lithium ions. After that, insertion becomes easier for the later ions. This observation has already been reported for crystalline V_2O_5 [22]. For XRGs, R_{ct} increased slowly with x at all lithium contents considered. So, in this case, no difficulty appeared for ion transfer in the host network; the interfacial properties were better than those of XRG.

4. Conclusion

Xerogels prepared with surfactant were found to have an insertion capacity of about 2.7 moles of lithium per mole of V_2O_5 . This value is superior to that in xerogels prepared without EON2 (1.6 Li/ V_2O_5 in that case) but is lower than previous results on spin-coating xerogels as reported by Park et al. [3]. The difference may be due to the more amorphous character of xerogels prepared with addition of the surfactant molecule. The two kinds of xerogels do not give the same intercalation sites, as shown by their cyclic voltammograms. The mechanisms of intercalation are also different in the two materials. Impedance measurements indicated different changes in insertion parameters (R_{ct} and D_{Li}) with x . The results demonstrate that the insertion of the first lithium ions into xerogels prepared without surfactant requires additional energy. This energy is necessary for structural rearrangement which then allows easier insertion for the subsequent Li^+ . For xerogels prepared with EON2, the behaviour is different since there is no difficulty for the

insertion of the first lithium ions. These insertion properties are probably due to the dilated structure of the new materials.

References

1. D.W. Murphy, P.A. Christian and N. Carides, *J. Electrochem. Soc.* **126** (1979) 497.
2. C.J. Brinker and G.W. Scherer, 'Sol-Gel Science' (Academic Press, San Diego, 1990).
3. H.K. Park, W.H. Smyrl and M.D. Ward, *J. Electrochem. Soc.* **142** (1995) 1068.
4. F. Chaput, B. Dunn, P. Fuqua and K. Salloux, *J. Non-Cryst. Solids* **11** (1995) 188.
5. D.B. Le, S. Passerini, X. Chu, D. Chang, B.B. Owens and W.H. Smyrl, *Electrochem. Soc. Proc* **94** (1996) 306.
6. J. Livage, *Solid State Ionics* **86** (1996) 935.
7. J. Livage, *Chem. Mater.* **3** (1991) 578.
8. E.Z. Muller, *Chem. Ind. Kolloide* **8** (1911) 302.
9. J. Livage, *Mater. Res. Soc. Symp. Proc.* **32** (1988) 125.
10. C. Sanchez, M. Nabavi and F. Taulelle, *Mater. Res. Soc. Symp. Proc* **121** (1988) 93.
11. D.C. Bradley, R.C. Mehrotra and D.P. Gaur, 'Metal Alkoxides' (Academic Press, London, 1978).
12. S. Mege, E. Perez, M. Verelst, P. Lecante, F. Ansart and J.M. Savariault, *J. Non Cryst. Solids* **238** (1998) 37.
13. M. Nabavi, C. Sanchez and J. Livage, *Eur. J. Solid State Inorg. Chem.* **28** (1991) 1173.
14. R. Enjalbert and J. Galy, *Acta Cryst.* **42** (1986) 1467.
15. S. Mege, Thesis, Université Paul Sabatier Toulouse France (1998).
16. Y. Maranushi, T. Kishi and T. Nagai, *Denki Kagaku* **53** (1985) 718.
17. J.E.B. Randles, *Discuss. Faraday Soc.* **1** (1947) 11.
18. J.R. Macdonald, 'Impedance Spectroscopy' (1987).
19. N. Kumagai, I. Ishiyama and K. Tanno, *J. Power Sources* **20** (1987) 193.
20. P.G. Dickens and G.J. Reynolds, *Solid State Ionics* **5** (1981) 331.
21. B. Zachau-Christiansen, K. West and Y. Jacobsen, *Solid State Ionics* **9** (1983) 399.
22. J. Farcy, R. Messina and J. Perichon, *J. Electrochem. Soc.* **137** (1990) 1337.